The Problem of Comparable GNSS Results – An Approach for a Uniform Dataset with Low-Cost and Reference Data

Pierre Reisdorf, Tim Pfeifer, *Julia Breßler, Sven Bauer, Peter Weissig, Sven Lange, Gerd Wanielik, Peter Protzel

Technische Universität Chemnitz
Reichenhainer Str. 70, 09126, Chemnitz, Germany
Email: firstname.lastname@etit.tu-chemnitz.de, *julia.bressler@wirtschaft.tu-chemnitz.de

***Abstract*—Localization and navigation are two key factors for our globalized world. Driven by cost-effective end-user devices, position estimation using Global Navigation Satellite Systems (GNSS) is common sense. Using the pseudorange measurements as input, many research groups developed their own approaches for estimating position information and evaluated it in simulation or real-world scenarios. Surprisingly, a common publicly available dataset for comparing such algorithms against each other has not been established. We pursue the idea of a uniform, free to use dataset collected by a low-cost receiver in conjunction with associated reference data originating from a high-precision device. For creating representative datasets, we chose four challenging scenarios within two different cities with various influences of urban canyons and surroundings. Based on this, we present first preliminary results from our Factor Graph approach. Our datasets are associated with the smartLoc project and are available online at: www.mytuc.org/GNSS**

Keywords–GNSS; Low-cost Sensor; NLOS; Reference Data; Urban Canyon

I. INTRODUCTION

Localization around the globe and in real time with satellites is a big accelerator to a globalized traffic and trade. The technique behind is called Global Navigation Satellite System (GNSS). In more detail, different satellite systems like the North American Global Positioning System (GPS), the Russian Glonass, the European Galileo or the Chinese BeiDou could be used for the localization process already. All these global systems and other local systems, like the Japanese QZSS (to mention just one), enable a fast localization under an open sky. However, satellite navigation is based on the transmission of electronic waves with its typical characteristics and drawbacks. That is, if we have a limited view to the sky, the localization process is faulty. Well-known examples are places in the proximity of high buildings or with dense and high vegetation. Hence, the localization process in urban scenarios was addressed by many research activities. Within urban areas, Non-line-of-sight (NLOS) and multipath are the largest challenges for an accurate and available position fix.

Existing research activities (see Table I) encounter these challenges in different ways with various approaches. All these activities base on simulated or real world data in static or dynamic scenarios [1]. Unfortunately, a major restriction of all published and founded work is the incomparability of the results. Thus, all existing works are only comparable with itself. It should be noted that the reasons for this fact could be diverse. That starts with additional sensors like cameras, light detection and ranging (LiDAR), radio detection and ranging (Radar), etc., special prepared maps with different content and ends with cooperative approaches to improve the position quality. To cover all the various approaches is impossible with one dataset. All approaches in context of GNSS use calculated position fixes or raw measurements (more known as pseudoranges) delivered by a receiver. At this point, we would like to publish a common dataset in typical scenarios, which addresses the mentioned challenges. We provide within this paper complete datasets with low-cost GNSS data, reference GNSS data, associated broadcasted ephemeris data, as well as ego motion data like yaw-rate and velocity. These datasets enable the user to calculate a position fix, compare with the reference data and fuse the data with ego motion output.

This paper is categorized in four main parts. After a brief introduction in the field of GNSS and a motivation to the question—*Why do we need a uniform dataset for GNSS data?*—a short state of the art overview regarding available datasets is shown. In the subsequent section, the methodology is introduced in detail. The following section presents the output data and explains each data type. In Section VI, we present first results from the project smartLoc [2]. The paper will end with a conclusion as well as an outlook. After all, the license terms for the given datasets will end the paper.

II. MOTIVATION

A major challenge of GNSS based systems in urban environments are NLOS measurements. These result from reflections of the received signals, which especially can occur in narrow streets between tall buildings, so-called urban canyons. Figure 1 shows such an urban canyon with the negative effects on the availability of satellites. For a better understanding of the challenges in the scene at hand, we added a sky plot (left side) with GPS (green) and Glonass (red) showing the reduced availability of satellites (in ideal view 16 satellites).

The common Kalman filter-based approach to fuse the measured pseudoranges uses a Gaussian distributed noise as error model. Through the geometrical elongation case of NLOS measurements, this error model becomes invalid, which leads to a large distortion of the position estimator. To prevent these distortions, the common filter approach has to be replaced with an algorithm that is better suited for non-Gaussian errors. For the simultaneous localization and mapping (SLAM) problem in robotics, a variety of robust optimization back-ends have been proposed in the recent past [3]–[10]. These back-ends can be applied to solve generic estimation problems like in GNSS

 ISBN: 978-1-61208-515-9

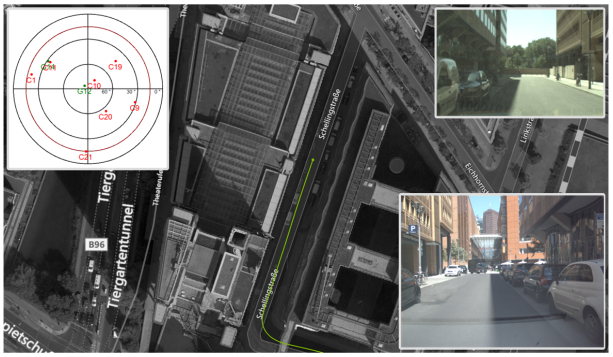

Figure 1. Birds eye view of an urban canyon including a front and rear view example (right side) from the scenario *Potsdamer Platz* in Berlin.

TABLE I. NUMBER OF PUBLICATIONS GROUPED BY ITS DATASET CHRACTERISTIC BASED ON [1]

Real Data collection	**Static measurement**	**Dynamic measurement**
Via vehicle	7	19
Via person	2	4
(No information)	11	—
Simulation	**Static measurement**	**Dynamic measurement**
Via vehicle	1	6
Via person	—	—
(No information)	4	

if they are formulated as factor graphs, a kind of Bayesian network. While for SLAM scenarios, multiple comparisons of robust graph optimization approaches like [11] and [12] exist, there are none for GNSS-related applications. For this reason, our first comparison in [13] was limited to synthetic data, but already showed the potential of this class of algorithms. To create a first foundation for a comparison under real world conditions, we decided to share the required data in form of a public available dataset, because none of the examined datasets (see Table I) fulfilled all our requirements in terms of surroundings and the necessary measurement data.

III. STATE OF THE ART

In science, it is necessary to compare various results against each other or to have a same base to build comparable conclusions. In the field of vision systems like training sets for different classifiers, there are serious datasets. For vision systems exist some databases, e.g., the Daimler Database for pedestrians [14] or the Nordland dataset [15] from a drive in a train over different seasons. In the field of mobile robotics, specifically SLAM, many real and synthetic datasets exist, like the well-known dataset of the Intel Research Lab. The spirit of providing datasets for competing algorithms is present in the community and online resources like [16], [17] or [18] provide collections of datasets and sometimes specific benchmarks for scoring results or more generic evaluations. Other datasets contain data about Naturalistic Driving Studies (NDS) from the project UDRIVE [19] and Strategic Highway Research Program 2 [20]. Another well-known source in the field of autonomous driving, including datasets and benchmarks, is the *Kitti Vision Benchmark Suite* [21] with focus on stereo processing, optical flow, visual odometry, object and lane detection and tracking. Still others focus on semantic understanding of urban street scenes like Cityscapes Dataset [22], different kind of published data from the INRIA Grenoble Rhône-Alpes team [23] or synthetic images of urban scenes [24]. The focus of all these datasets are different from a dataset addressed for the GNSS field (raw measurements and reference data). In our view the conditions of a uniform dataset are:

- Low-cost GNSS position
- Smoothed Reference GNSS position
- Odometry data (yaw-rate and velocity)
- Ephemeris data

Some datasets contain localization information, but neither includes precise data as well as low-cost data. The focus of the majority of the introduced datasets are vision systems. At this point, we would like to fill the gap with real data from urban scenarios including low-cost GNSS data and an associated reference data.

IV. METHODOLOGY

In this section, we describe in detail all conditions to the data recording procedure used to create the four proposed datasets located in Frankfurt/Main and Berlin. Ground-truth information is generated in post-processing mode, as described later on. It is based on the high-precision reference system's measurements.

A. Precondition on Data

After the taxonomy of the multipath/NLOS problem by [25] there are some preconditions to the kind of data. Different approaches use external map data as an additional sensor. Other approaches use *Quality parameters* like Signal-noise-ratio, Doppler frequency or Carrier phase. Still others use additional sensors like camera, laser or radar for data fusion approaches. No dataset is able to cover all possible setups. Hence, we focus on a good selection of the measurement tracks, where data for buildings and environments are available. For Berlin, there is public data in the project *Berlin 3D* [26] available. For the city of Frankfurt am Main, the *Stadtvermessungsamt* [27] published some inner city data. Likewise, the open project osm-3D [28] provides city data, but for many cities. The above mentioned quality parameters are supported by our low-cost receiver. They are included within our data accordingly. However, as the current work has its focus on GNSS-based position estimation, we neglect camera data for now, even if we have recorded some. The dataset is recorded with our test vehicle Carai1, which will be described later on.

B. Measurement Tracks

Based on the aspects detailed above, we examined possible environments suiting our demands for a challenging dataset. Especially, we focused on Urban Canyons, where NLOS and multipath are present to a large extend. Looking for a suitable route, we first extracted the cities, which have a large amount of high-rise buildings. Thus, we identified the cities of Frankfurt/Main and Berlin. We designed our test tracks to lie preferably within areas with high-rise and densely populated buildings as well as narrow streets. Naturally, these properties are met more or less during one scenario. An overview of all four scenarios with its tracks is given in Figure 4.

Within the city of Berlin, we located one track around the *Potsdamer Platz* (Scenario 1). It has a length of about 1.6 km

 ISBN: 978-1-61208-515-9

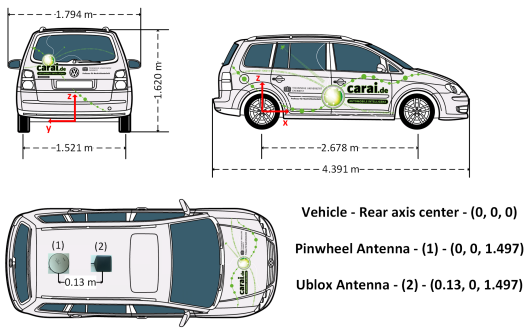

Figure 2. Schematic view in all dimensions of our test vehicle Carai1.

and is accompanied with 70 m to 100 m high buildings (Forum Tower, Kollhoff Tower, etc.). The road width varies between 13 m to 17 m and according to the approach in Sec. IV-F, we got 49 % NLOS measurements. The example view of an *Urban Canyon* in Fig. 1 originates from this scenario. The second track within Berlin is centered around the Friedrichstrasse and is referred to as *Gendarmenmarkt* (Scenario 2). The track is roughly 5 km long and includes 13 blocks. The streets are framed by 20 m to 60 m high buildings and the road width is about 20 m to 23 m. Here we have an NLOS ratio of about 37 %.

Within the city Frankfurt am Main, the first track is referred to as *Main Tower* (Scenario 3), which includes the highest tower of Germany. Here, the Urban Canyon is characterized by 110 m to 259 m high buildings. The route is about 3 km long with 46 % NLOS measurements. The second track within Frankfurt is called *Westend Tower* (Scenario 4), which includes three high-rise buildings (208 m, 200 m, 142 m). The track is measured to 2.3 km and the road width varies between 10 m to 70 m while the NLOS ratio is about 32 %.

C. Sensor Setup

We use both a high-cost GNSS sensor (for reference or ground truth position) and a low-cost GNSS sensor for localization. Additionally, we recorded odometry data (yaw-rate and velocity) from the test vehicle Carai1 [29]. The low-cost data can be divided in two categories. On the one hand side calculated position fixes and on the other hand side raw measurements. We get the reference position as a calculated position fix from the NovAtel sensor. Table II describes the sensors, which were used during the recording process. All GNSS sensors are market products without any adaption from our side.

TABLE II. SENSORS FOR RECORDING

Sensor	*Description*
1) Low-cost GNSS sensor	u-blox EVK-M8T (u-blox M8 GNSS Evaluation Kit *Precision Timing*) with ANN-MS antenna
2) Reference GNSS sensor	NovAtel SPAN Differential (Model CDJRPRT-TNS2) GPS, GLO, BeiDou with RTK and IGM-S1 Inertial Measurement Unit (IMU) and Pinwheel-Antenna (Model GPS-703-GGG [30])
3) Odometry	For obtaining ego motion data over the CAN gateway.
4) Carai1	One of our three test vehicle equipped with different sensors [29]. This test vehicle is a VW Touran.

The positions of the antennas on top of the roof of our test vehicle Carai1 [29] are shown in Figure 2. The figure illustrates the schematic view of all antennas. The Pinwheel antenna is mounted 1.497 m above the origin of the vehicle coordinate system. The centers of antenna one and antenna two are on the same height. All units in this figure are in meter. By virtue of a firmware update of the u-blox sensor during the both measurement campaigns, we have a different availability of satellite systems in the scenarios. Table III shows the different constellation for each scenario in Berlin and Frankfurt.

TABLE III. SATELLITE SYSTEMS IN SCENARIOS AT GLANCE

Satellite system	*GPS*	*GLO*	*GAL*
Potsdamer Platz	x	x	
Gendarmenmarkt	x	x	
Main Tower	x	x	x
Westend Tower	x	x	x

D. Procedure of Sensor Data

Our software base for recording, processing and analysis of the data are the system development framework vADASdeveloper by Vector [31] and the sensor fusion development library BASELABS Create [32]. We divide our procedure to handle and processing the data in three steps. Figure 3 illustrates these three steps, which are necessary to get a complete comparable dataset.

1) Record real data during a measurement campaign
2) Post processing the data for generating of ground truth
3) Generation of export data

Step one consists of both recording the data and check the data for consistency of the desired recording setup. Step two contains the processing of all data and create a ground truth for each position related data to export. The last step generates the export data in form of different *Character Separated File (CSV)* files.

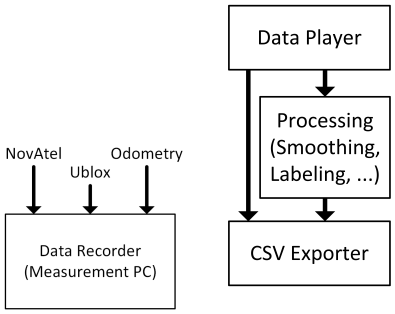

(a) Recording (b) Post processing and export

Figure 3. Schematic representation of the procedure for recording, post processing and generation of export data.

Which messages from the sensors did we recorded? Table IV gives an overview about the messages with the associated frequency for each sensor. For more details, take a look into the manuals of the sensor (u-blox [33] and [34], NovAtel without IMU [35] and with IMU [36]). The log type indicates the type of a messages, continuous or when a new message available. The messages BestPos and BestVel from NovAtel can used for the generation of ground truth and is also a part of the exported data.

A worldwide common coordinate system for localization is the World Geodetic System 1984 (WGS 84). A definition

 ISBN: 978-1-61208-515-9

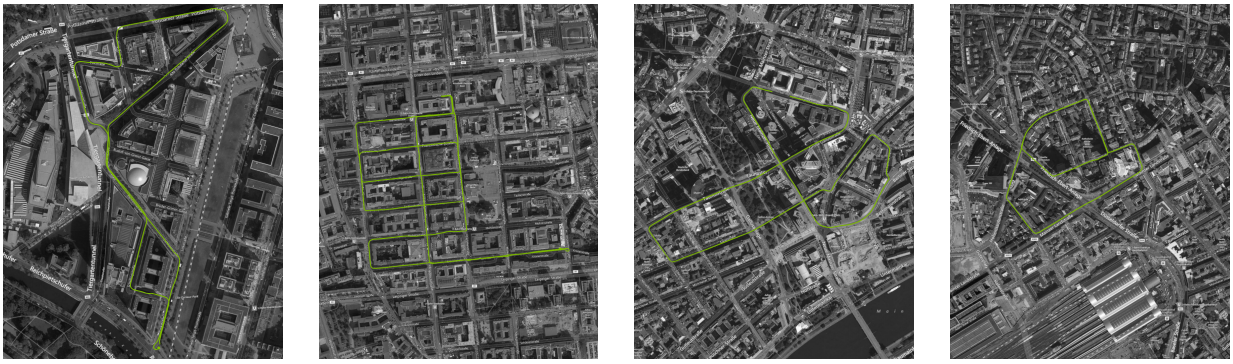

(a) Berlin 1 - Potsdamer Platz (b) Berlin 2 - Gendarmenmarkt (c) Frankfurt 1 - Main Tower (d) Frankfurt 2 - Westend Tower

Figure 4. Aerial view of the selected scenarios. We chose two different tracks (visualized as green line) in the city of Berlin and Frankfurt am Main (Germany). They are representative examples for a so called *Urban Canyon*.

TABLE IV. DATA FROM SENSORS

Sensor	*Data type*	*Log type*	*Frequency (Hz)*
Low-cost GNSS sensor	NAV-POSLLH	Sync	5
	RXM-RAWX	Sync	5
High-cost GNSS sensor	BESTPOS	Sync	20
	BESTVEL	Sync	20
Odometry	YAWRATE	Sync	50
	VELOCITY	Sync	50

of the WGS 84 system is done by the National Imagery and Mapping Agency [37] or in the *Global Positioning System Standard Positioning Service Signal Specification* [38]. This coordinate system can be called as the standard coordinate system and all our position information refer to it.

E. Parameters for Data

This section includes some explanations and details about the exported data. In detail, some hints about the time format, the ground truth format as well as both ephemeris data formats for GPS and Glonass.

GPS time: The first and second column of each exported data file describe the GPS time. This time is the measurement time on the sensor side. The GPS time is divided into the GPS week (first column) and the GPS seconds of week (second column). More explanations to GPS time in section V-C.

Ground truth: The base of our provided ground truth is BestPos message from NovAtel sensor [35] and odometry data (velocity and yaw-rate). Hence, the coordinate system is WGS 84 in the format of Longitude, Latitude and Height (above mean sea level) too. In subsection V-C there are more details and explanations about the ground truth.

Ephemeris data: For a complete set of data, we use the ephemeris data from the German Research Centre for Geosciences (GFZ) [39], which provide data to the Multi-GNSS EXperiment (MGEX) of the International GNSS Service (IGS). This service provides orbit data in the Extended Standard Product 3 Orbit Format (SP3) for the most common satellite systems in Europe. SP3 format is a standard format in GNSS field and gives a fast access to this data without any special adaptions.

F. Label for LOS/NLOS

The NovAtel receiver is also able to provide raw measurement (pseudorange) information like the u-blox receiver. The u-blox receiver provide information about all received satellite signals. The NovAtel receiver seems to exclude some satellites in harsh environments, which might be affected by NLOS. NovAtel used for receiving a Pinwheel antenna and internally different algorithms. Hence, we use this information to build a NLOS detection based on different satellites availabilities in both receivers. Therefore, we remember the last received set of satellites from NovAtel and time of data. When we receive in next step a set of satellites from u-blox, we compare the availability of each satellite and time span since the last update from the NovAtel. If the time span is too high or the satellite was never seen before, the pseudorange measurement or satellite marked as NLOS. In the other case, the measurement marked as LOS. This approach gives a hint for the type of LOS or NLOS of a given measurement and we export this information to complete the datasets.

V. OUTPUT OF DATA

This section describes in the first part the structure of the data and gives some comments for a fast implementation of an importer for the data. The second part explains in more detail the creation of the ground truth data, which is the base for a comparison of each algorithm based on the low-cost data.

A. Structure of Exports

There are six message types, which are exported in separate files. The name of the messages and the log type as well as the frequency are described in Table IV. Additionally, the SP3 file is provided by the GFZ and we add this to our exports. All exports have the same structure and the delimiter used in the CSV-files are semicolons. Each line starts with the measurement GPS time of the sensor, followed by the structure described in the data manuals. Additionally, the exports for the messages NAV-POSLLH and RXM-RAWX have information about the ground truth included – more details are described in Section V-C. That means, the structure of both file types follows this structure:

NAV-POSLLH and RXM-RAWX: GPSWeek; GPSSeconds; GTLongitude; GTLongitude Cov; GTLatitude; GTLatitude Cov; GTHeight; GTHeight Cov; GTHeading; GTHeading Cov;

 ISBN: 978-1-61208-515-9

GTAcceleration; GTAcceleration Cov; GTVelocity; GTVelocity Cov; GTYawRate; GTYawRate Cov; next entries followed by manual for each message... GT means in this context ground truth.

Other exports: GPSWeek; GPSSeconds; next entries followed by manual for each message...

One full export of a scenario consists of the following data files (same order like in Table IV):

1) NAV-POSLLH.csv
   A Geodetic Position Solution calculated by the low-cost receiver.
2) RXM-RAWX.csv
   Multi-GNSS raw measurements for GPS and Glonass from the low-cost receiver.
3) YAWRATE.csv
   Yaw-rate data from the ego motion sensor of the test vehicle Carai1.
4) VELOCITY.csv
   Velocity data from the ego motion sensor of the test vehicle Carai1.
5) SP3 file
   Includes the post-processed ephemeris data for all relevant satellite systems.
6) BESTPOS.csv and BESTVEL.csv
   The BestPos is the raw ground truth message from the reference system. We use this message for our smoothing process to build the post-processed ground truth. The BestVel includes best available velocity data from the reference system.

All datasets are published under Creative Commons Attribution-NonCommercial-ShareAlike 4.0 license on the project website of smartLoc – http://mytuc.org/GNSS. A complete package of each message types for all scenarios is available there.

B. Challenges of selected scenarios

As described in section IV-B, we have decided us for urban scenarios with harsh environments for satellite reception. The challenges are the ever changing satellite availabilities. To get a better understanding of NLOS influence in urban areas, we chose the fourth scenario (Westend Tower) to show some details. In Figure 5, two diagrams are shown to visualize the challenge within this urban canyon. The lower diagram shows the theoretically possible number of satellites currently visible in relation to the satellites classified as NLOS. Accordingly, the upper diagram shows the NovAtel receiver's estimated standard deviation. It is easy to see, that if the number of NLOS measurements is increasing, the estimated accuracy is decreasing in consequence. Indeed, we have situations with less than four LOS satellites. Thus, the IMU supports the reference system to stabilize the localization. This is important to note and restricts the quality of the assumed ground truth originating from the receivers BestPos messages. Later on, we describe how to support the ground truth by post-processing it with a smoother and additional odometry information. All other recorded scenarios show the same effects between NLOS and standard deviation of the reference system.

C. Merge all Data - Smoothing

During the measurement campaigns multiple sensors were used. In detail, the sensor output of a u-blox EVK-M8T low-cost GNSS receiver, a NovAtel INS SPAN reference GNSS system and the vehicle's odometry has been recorded. As the sensors are not synchronized, we have to align them first to a common timescale, before using them as input to our smoothing algorithm.

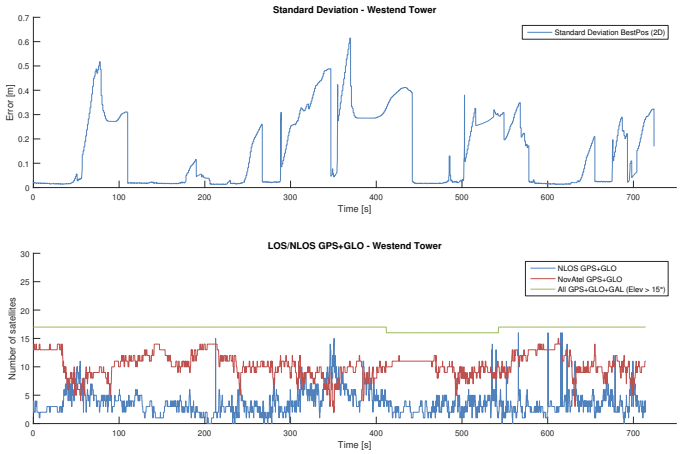

Figure 5. Influence of satellite numbers and NLOS to standard deviation of BestPos message from reference system. The number of NLOS was created after the strategy described in section IV-F. Both diagrams show the Frankfurt Westend Tower scenario.

The given system timestamp of each measurement denotes the time of arrival according to the computer's system clock. The NovAtel and u-blox measurements also include the actual time of measurement in GPS time. As the computer clock is quite unstable in general and the timestamping is also influenced by variable delays due to the operating system's thread scheduling, the time of arrival jitters a lot. To get the highest quality ground truth, the data fusion has been performed using GPS time as the reference. As the vehicles odometry sensor lacks a GPS timestamp, it has been estimated as follows:

- Estimate the relation between NovAtels GPS time of measurement and time of arrival.
- Estimate the relation between an idealized odometry time of measurement and time of arrival.
- Combine the two relations to transform the idealized time of measurement to GPS time.
- Correct the time offset to account for different processing delays.

In the first step the NovAtels GPS time of measurement was compared to the time of arrival, estimating the bias and drift between both clocks using a first order polynomial curve fit.

Following this, a stable internal clock that triggers odometry measurements every $20\,\mathrm{ms}$ was assumed for the odometry sensor. An idealized hardware timestamp was computed for each odometry measurement as the product of the measurements successive number and this period time. This hardware timestamp was then related to the time of arrival the same way as the NovAtels GPS time before. This yielded the bias and drift between the idealized measurement time and the computers system time.

Combining these two relations allowed then the computation of the odometries apparent period time within the GPS timescale and its time offset, so suitable GPS timestamps could be derived.

 ISBN: 978-1-61208-515-9

At last, the time offset needed to be adjusted as the previous steps implicitly assumed that both sensors have the same time delay between taking the measurement and applying the system timestamp. An optimizer was used to tune the time offset minimizing the average error between the odometries and NovAtels velocity measurements. As a second optimization parameter, the odometries velocity scaling error was determined too. This scaling error is caused by a changed wheel diameter due to tire wear in respect to the wheel diameter that the revolution counter assumes.

Finally, a Rauch-Tung-Striebel smoothing filter is applied, which uses an unscented Kalman filter in a two-way-smoothing fashion. It used a constant turn-rate and acceleration (CTRA) motion model to estimate the vehicle movement. This motion model was chosen as it is one of the most advanced curvilinear motion models commonly used for vehicle state estimation. Further improvements – like the constant curvature and acceleration model (CCA) – offer only minor benefits but lead to fresnel integrals requiring numerical approximations increasing the implementation complexity and computational cost. More commonly, even simpler motion models like a constant turn-rate and velocity (CTRV) or even constant velocity (CV) are used. As their respective state spaces are subsets of the CTRA state space, smoothing using the CTRA model creates a ground truth that allows the evaluation of those as well.

TABLE V. PROCESS NOISE PARAMETERS USED BY THE CTRA MODEL BASED FILTERS

Parameter	*Value*
Angular acceleration	0.2 rad/s
Jerk	2.0 m/s^3
Altitude acceleration	0.04 m/s^2
Yaw-rate bias drift	0.0001 rad/s

A comparison of the mentioned motion models including their basic state space definitions and state transition equations can be found in [40]. Extending this, the CTRA model has been augmented to use 3D coordinates. While the original horizontal position estimation was left unchanged, the positions Z component was added as well as an additional altitude velocity to model the altitude assuming a constant climb rate. To optimally include the odometry measurements, the scaling error that had been estimated by the optimizer during the time synchronization process is applied within the odometry velocity measurement model. The odometry yaw-rate bias, however, was estimated online by the filter assuming it to be constant. The used noise parameters for the resulting process model are shown in Table V. The angular acceleration and jerk being noises for the otherwise constant turn-rate and acceleration, the altitude acceleration for the constant altitude velocity and drift for the estimated yaw-rate bias.

VI. FACTOR GRAPH OPTIMIZATION

In the following section we want to give an example of the result of state-of-the-art algorithms with the provided dataset. For the estimation of a trajectory based on a set of pseudo-ranges, a sensor fusion algorithm has to be applied. Similar to our former benchmark [13], we use a factor graph as graphical representation of a non-linear least squares minimization problem. In its general topology the same graph as proposed in [41] is used, including atmospheric (Ionosphere and Troposphere) and satellite clock corrections. The robust

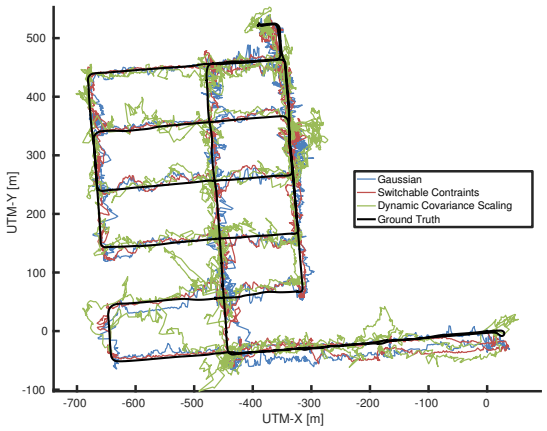

Figure 6. Resulting trajectory of an online factor graph optimization with the GTSAM library for the Berlin Gendarmenmarkt dataset.

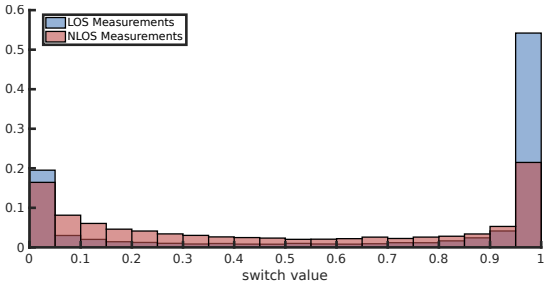

Figure 7. Normalized distribution of the switch variables of the switchable constraints algorithm for the Berlin Gendarmenmarkt dataset. These weights should be 1 for LOS measurements an 0 for NLOS, if the algorithms works perfect.

algorithms Switchable Constraints (SC) [3] and Dynamic Covariance Scaling (DCS) [4] were implemented within the GTSAM framework [42] and solved online with the provided iSAM2 algorithm [43]. For further algorithmic details, we refer to our earlier descriptions in [13] or the original papers of each algorithm. A constant position model is used to avoid the more complex handling of the odometry, which has a different measurement rate than the satellite system.

The estimated trajectory of the Berlin Gendarmenmarkt data stream at Figure 6 shows the strong distortion that is most likely caused by NLOS Observations. Table VI summarizes the 2-dimensional UTM-X/Y position error for all data streams. This error can be described as the Euclidean distance between the estimated position and the ground truth. Similar to our former comparison at high NLOS ratios, the DCS algorithm shows bad results. The high NLOS amount over 30% in combination with the lack of odometry could be the reason for the insufficient performance of this algorithm. Especially with the missing odometry and the simplified motion model, there is no possibility to set the new initial position values different from the previous ones. Such a suboptimal initialization can be a problem for robust algorithms, like shown in [44] or [45].

Switchable Constraints on the other side is able to improve the position estimate over the results of the pure Gaussian factor graph. Nevertheless, is the improvement smaller than we would expect based on our former work. To investigate the problem of the SC algorithm, we visualized the switch values, a kind of continuous weights for each measurement, with Figure

 ISBN: 978-1-61208-515-9

TABLE VI. RESULT OF THE FACTOR GRAPH BASED POSITION ESTIMATION

	Gaussian			Switchable Constraints			Dynamic Covariance Scaling		
	Absolute Position Error [m]								
Dataset	mean	median	max	mean	median	max	mean	median	max
Berlin Potsdamer Platz	23.70	21.16	72.24	25.11	19.89	78.17	32.92	25.05	111.4
Berlin Gendarmenmarkt	17.04	15.86	62.90	15.32	13.06	54.21	22.84	19.26	118.5
Frankfurt Main Tower	19.68	12.74	158.1	18.02	10.32	137.9	61.95	29.50	763.1
Frankfurt Westend Tower	16.10	11.86	105.2	14.57	10.43	90.41	32.30	11.68	284.0

7. A perfect distribution would show all LOS values on the right side around 1 and all NLOS values around 0 at the left. Although the NLOS values are more on the left side than the LOS one, the histogram is far from ideal. So, a high amount of NLOS pseudoranges is included in the optimization process, which explains the results. However, for final conclusions about the performance of robust algorithms on these datasets there is still a lot to do.

VII. CONCLUSION & OUTLOOK

Challenging datasets for the evaluation and application of GNSS based position estimation algorithms have been presented in this work. The selected tracks cover ordinary situations typically encountered in urban environments, such as limited satellite visibility, uncounted reflections and satellite signal outages caused by buildings. As our aim is the reusability of our dataset for the evaluation of competing algorithms within the GNSS field, we gave detailed information about our experimental setup as well as an analysis of our datasets including a description of the provided file types.

The included results of a factor graph based position estimation provide a first baseline to compare future implementations. For further improvements, the online estimation of the underlying error distribution seems to be an important next step. With a good representation of this distribution, we will be able to apply other robust sensor fusion algorithms like Max-Mixture [9] or generalized iSAM [46]. Also, we have to invest more efforts to characterize the error distribution of this dataset and the differences to our previous synthetic test.

Another point is the handling of information inside the datasets. Currently, some expert knowledge is needed for extracting the satellite positions from the SP3 file or to estimate different errors, e.g., ionospheric or tropospheric delays, which influence the accuracy of the ego position result. The extension of our datasets for such information facilitate the access to the information inside the dataset.

Within varying published work, some approaches use camera information for NLOS detection [47], traffic sign recognition for additionally landmarks [48] or lane mark recognition to stabilize the localization [49], to address just some examples. Due to publishing camera information, the dataset could be more interesting for variety of other approaches using camera information.

ACKNOWLEDGMENT

This evaluation was done as part of the smartLoc project, which is funded by the "Bundesministerium für Wirtschaft und Energie" (German Federal Ministry for Economic Affairs and Energy). For this evaluation and generation of ground truth data, precise real-time corrections provided by the AXIO-NET service (www.axio-net.eu) were used.

REFERENCES

[1] J. Breßler, P. Reisdorf, M. Obst, and G. Wanielik, "Gnss positioning in non-line-of-sight context - a survey," 2016, manuscript submitted for publication at 19th International IEEE Conference on Intelligent Transportation Systems (ITSC).

[2] Retrieved: Sept. 2016. [Online]. Available: https://www.smartLoc.eu/

[3] N. Sünderhauf, "Robust optimization for simultaneous localization and mapping," Ph.D. dissertation, Technischen Universität Chemnitz, 2012.

[4] P. Agarwal, G. D. Tipaldi, L. Spinello, C. Stachniss, and W. Burgard, "Robust map optimization using dynamic covariance scaling," in Proc. of Intl. Conf. on Robotics and Automation (ICRA), 2013, pp. 62 – 69.

[5] P. Agarwal, G. Grisetti, G. Diego Tipaldi, L. Spinello, W. Burgard, and C. Stachniss, "Experimental analysis of dynamic covariance scaling for robust map optimization under bad initial estimates," in Proc. of Intl. Conf. on Robotics and Automation (ICRA), 2014, pp. 3626 – 3631.

[6] P. Agarwal, "Robust graph-based localization and mapping," Ph.D. dissertation, PhD thesis, University of Freiburg, Germany, 2015.

[7] Y. Latif, C. Cadena, and J. Neira, "Robust loop closing over time for pose graph slam," The International Journal of Robotics Research, vol. 32, no. 14, 2013.

[8] G. H. Lee, F. Fraundorfer, and M. Pollefeys, "Robust pose-graph loop-closures with expectation-maximization," in Proc. of Intl. Conf. on Intelligent Robots and Systems (IROS), 2013, pp. 556 – 563.

[9] E. Olson and P. Agarwal, "Inference on networks of mixtures for robust robot mapping," The International Journal of Robotics Research, vol. 32, no. 7, 2013, pp. 826–840.

[10] D. M. Rosen, M. Kaess, and J. J. Leonard, "Robust incremental online inference over sparse factor graphs: Beyond the gaussian case," in Proc. of Intl. Conf. on Robotics and Automation (ICRA), 2013, pp. 1025 – 1032.

[11] N. Sünderhauf and P. Protzel, "Switchable constraints vs. max-mixture models vs. rrr – a comparison of three approaches to robust pose graph slam," in Proc. of Intl. Conf. on Robotics and Automation (ICRA), 2013, pp. 5198 – 5203.

[12] Y. Latif, C. Cadena, and J. Neira, "Robust graph SLAM back-ends: A comparative analysis," in Proc. of Intl. Conf. on Intelligent Robots and Systems (IROS), 2014, pp. 2683 – 2690.

[13] T. Pfeifer, P. Weissig, S. Lange, and P. Protzel, "Robust factor graph optimization – a comparison for sensor fusion applications," in Proc. of Intl. Conf. on Emerging Technologies and Factory Automation (ETFA), 2016.

[14] Retrieved: Sept. 2016. [Online]. Available: http://www.gavrila.net/Datasets/datasets.html

[15] Retrieved: Sept. 2016. [Online]. Available: http://www.nrkbeta.no/2013/01/15/nordlandsbanen-minute-by-minute-season-by-season/

[16] Retrieved: Sept. 2016. [Online]. Available: http://radish.sourceforge.net

[17] S. Ceriani, G. Fontana, A. Giusti, D. Marzorati, M. Matteucci, D. Migliore, D. Rizzi, D. G. Sorrenti, and P. Taddei, "Rawseeds ground truth collection systems for indoor self-localization and mapping," Autonomous Robots, vol. 27, no. 4, 2009, pp. 353–371.

[18] Retrieved: Sept. 2016. [Online]. Available: http://projects.asl.ethz.ch/datasets

[19] Retrieved: Sept. 2016. [Online]. Available: http://www.udrive.eu/

[20] Retrieved: Sept. 2016. [Online]. Available: https://insight.shrp2nds.us/

[21] Retrieved: Sept. 2016. [Online]. Available: http://www.cvlibs.net/datasets/kitti/

[22] Retrieved: Sept. 2016. [Online]. Available: https://www.cityscapes-dataset.com/

 ISBN: 978-1-61208-515-9

[23] Retrieved: Sept. 2016. [Online]. Available: http://lear.inrialpes.fr/data

[24] G. Ros, L. Sellart, J. Materzynska, D. Vazquez, and A. Lopez, "The synthia dataset: A large collection of synthetic images for semantic segmentation of urban scenes," in IEEE Conference on Computer Vision and Pattern Recognition, 2016.

[25] M. Obst, "Bayesian Approach for Reliable GNSS-based Vehicle Localization in Urban Areas," Ph.D. dissertation, Technische Universität Chemnitz, 2015.

[26] Retrieved: Sept. 2016. [Online]. Available: http://www.businesslocationcenter.de/en/downloadportal

[27] Retrieved: Sept. 2016. [Online]. Available: https://www.frankfurt.de/sixcms/detail.php?id=3027

[28] Retrieved: Sept. 2016. [Online]. Available: http://www.osm-3d.org/

[29] R. Schubert, E. Richter, N. Mattern, P. Lindner, and G. Wanielik, Advanced Microsystems for Automotive Applications 2010 - Smart Systems for Green Cars and Safe Mobility. Springer, 2010, ch. A Concept Vehicle for Rapid Prototyping of Advanced Driver Assistance Systems, pp. 211 – 219.

[30] GPS-703-GGG and GPS-703-GGG-N User Guide, 4th ed., NovAtel, April 2014.

[31] Retrieved: Sept. 2016. [Online]. Available: http://www.vector.com/vi_vadasdeveloper_en.html

[32] Retrieved: Sept. 2016. [Online]. Available: https://www.baselabs.de/data-fusion-algorithm-design/

[33] U-blox 6 Receiver Description, GPS.G6-SW-10018-F ed., u-blox, April 2013.

[34] U-blox 8 / u-blox M8; Receiver Description; Including Protocol Specification, R10 (111670) ed., u-blox, February 2016.

[35] OEM6 Family of Receivers - Firmware Reference Manual, 9th ed., NovAtel, March 2016.

[36] SPAN® on OEM6® Firmware Reference Manual, 7th ed., NovAtel, January 2015.

[37] National Imagery and Mapping Agency, "Department of Defense World Geodetic System 1984: its definition and relationships with local geodetic systems," National Imagery and Mapping Agency, St. Louis, MO, USA, Tech. Rep. TR8350.2, January 2000. [Online]. Available: http://earth-info.nga.mil/GandG/publications/tr8350.2/tr8350_2.html

[38] Global Positioning System Standard Positioning Service Signal Specification, 2nd ed., United States Coast Guard Navigation Center, Juni 1995. [Online]. Available: http://www.navcen.uscg.gov/pubs/gps/sigspec/gpssps1.pdf

[39] M. Uhlemann, G. Gendt, M. Ramatschi, and Z. Deng, GFZ Global Multi-GNSS Network and Data Processing Results. Cham: Springer International Publishing, 2016, pp. 673–679. [Online]. Available: http://dx.doi.org/10.1007/1345_2015_120

[40] R. Schubert, E. Richter, and G. Wanielik, "Comparison and evaluation of advanced motion models for vehicle tracking," in Information Fusion, 2008 11th International Conference on, June 2008, pp. 1–6.

[41] N. Sünderhauf, M. Obst, S. Lange, G. Wanielik, and P. Protzel, "Switchable constraints and incremental smoothing for online mitigation of non-line-of-sight and multipath effects," in Proc. of Intelligent Vehicles Symposium (IV), 2013.

[42] Retrieved: Sept. 2016. [Online]. Available: https://collab.cc.gatech.edu/borg/gtsam

[43] M. Kaess, H. Johannsson, R. Roberts, V. Ila, J. J. Leonard, and F. Dellaert, "isam2: Incremental smoothing and mapping using the Bayes tree," Intl. Journal of Robotics Research, vol. 31, no. 2, Dec. 2012, pp. 216–235.

[44] D. M. Rosen, C. DuHadway, and J. J. Leonard, "A convex relaxation for approximate global optimization in simultaneous localization and mapping," in 2015 IEEE International Conference on Robotics and Automation (ICRA), May 2015, pp. 5822–5829.

[45] J. Wang and E. Olson, "Robust pose graph optimization using stochastic gradient descent," in 2014 IEEE International Conference on Robotics and Automation (ICRA), May 2014, pp. 4284–4289.

[46] D. M. Rosen and J. J. Leonard, "Nonparametric Density Estimation for Learning Noise Distributions in Mobile Robotics," in Workshop on Robust and Multimodal Inference in Factor Graphs, ICRA, 2013.

[47] P. D. Groves, Z. Jiang, M. Rudi, and P. Strode, "A Portfolio Approach to NLOS and Multipath Mitigation in Dense Urban Areas," in Proceedings of the 26th International Technical Meeting of The Satellite Division of the Institute of Navigation (ION GNSS 2013), 2013, pp. 3231 – 3247.

[48] A. Welzel, P. Reisdorf, and G. Wanielik, "Improving urban vehicle localization with traffic sign recognition," in 2015 IEEE 18th International Conference on Intelligent Transportation Systems, Sept 2015, pp. 2728–2732.

[49] N. Mattern, M. Obst, R. Schubert, and G. Wanielik, "Simulative analysis of accuracy demands of co-operative localization in the COVEL project," in Intelligent Vehicles Symposium (IV), 2011 IEEE, June 2011, pp. 516 – 521.

 ISBN: 978-1-61208-515-9